

Fall 2018

Nanoparticles and Their Use in Cancer Imaging, Prevention and Treatment

George Gray

Follow this and additional works at: <https://pillars.taylor.edu/chemistry-student>

 Part of the [Analytical Chemistry Commons](#), [Inorganic Chemistry Commons](#), [Organic Chemistry Commons](#), [Other Chemistry Commons](#), and the [Physical Chemistry Commons](#)

Recommended Citation

Gray, George, "Nanoparticles and Their Use in Cancer Imaging, Prevention and Treatment" (2018). *Student Scholarship: Chemistry*. 14. <https://pillars.taylor.edu/chemistry-student/14>

This Thesis is brought to you for free and open access by the Chemistry and Biochemistry at Pillars at Taylor University. It has been accepted for inclusion in Student Scholarship: Chemistry by an authorized administrator of Pillars at Taylor University. For more information, please contact pillars@taylor.edu.

Nanoparticles and Their Use in Cancer Imaging, Prevention and Treatment

George Gray

Senior Chemistry Thesis

December 7, 2018

Introduction:

Chemists are constantly searching for solutions to various problems and one of the solutions that has become popular to turn to is the nanoparticle. A nanoparticle is defined as a particle with dimensions between 1 and 100 nanometers. These tend to be surrounded by an interfacial layer that plays an integral part in the properties of the particles. Nanoparticle chemistry gained momentum in the 1980s and has become a major topic in the chemical research field. Many uses have been found for nanoparticles as they offer unique variability. The ability to control the size, shape, exterior composition and cargo make them ideal solutions for many problems. They have been used to help stabilize food emulsions,¹ create vaccinations,² and clean up water produced from fracking.³ One of the major fields that has been greatly expanding is the department of nanomedicine. Since nanoparticles are small enough to travel throughout various parts of the cell, they accumulate well within cells. Much of the current research in nanoparticles is directed toward the use of nanoparticles for cancer treatment, prevention and imaging.

Cancer is a set of diseases in which abnormal cells divide without control and have the ability to invade nearby tissues.⁴ Most of the popular treatments used today involve organometallics, immunotherapy and radiation. One of the most common and well known treatments is an organometallic known as cisplatin.⁵ This treatment makes use of a platinum-based compound to destroy cancer cells, but a common problem is getting treatments such as this to the cancer cells. Nanoparticles offer a unique tunability that makes them great carriers for cancer treatments that can surpass some of the many obstacles within the body and deliver the treatment to the desired cancer cells. Nanoparticles can be used in imaging, prevention and treatment of cancer. The four nanoparticles that will be examined here have been developed for one or more of these three uses.

Iron Oxide Nanoparticle for Use as a Magnetic Resonance Contrast Agent

Superparamagnetic iron oxide nanoparticles (SPION) have been a topic of interest for many chemists within the cancer related nanoparticle field. This is because of the potential that has been displayed in applications such as drug delivery, therapy, and magnetic resonance imaging (MRI).⁶ The common contrast agents required for MRI are gadolinium-based. SPION has the potential to replace these gadolinium-based contrast agents as they may offer a higher enhancement of imaging. The direct use of SPION as an MRI contrast agent results in the formation of aggregates within the blood plasma and are quickly removed by macrophages.⁷ Macrophages are a type of white blood cell that digests foreign substances within the body. This problem with SPION seems to be caused by the high surface-to-volume ratio and the forces between the nanomagnetites. The hope of Lee, *et al.* was to engineer a SPION with a surface that could minimize the aggregation of the particles within normal physiological conditions.⁸

Various polymers have been used to modify the surface of the SPION to increase their ability to function *in vivo*. Poly(ethyleneglycol)s (PEG) has been widely used with success, but there is concern about the stability of the PEG coat in physiological conditions since the PEG coating has typically been achieved through noncovalent interactions between the PEG and the surface of the nanoparticle. To correct for this concern, Lee, *et al.* took the approach of forming polymeric monolayers of PEG-silane copolymers via covalent bonds to the SPION. The copolymer used was poly(TMSMA-*r*-PEGMA). This is a randomized copolymer synthesized from (trimethoxy silyl)propyl methacrylate and PEG methacrylate.⁹ Adding the copolymer to the SPION created a poly(TMSMA-*r*-PEGMA)-coated SPION or poly(TMSMA-*r*-PEGMA)@SPION.⁸

To produce the polymer-coated SPION, two methods can be used. The iron oxide core is formed and separated while the polymer is being added or the polymer is added after the core nanoparticle is formed. The former version was labeled as “in situ” (IS) and the latter as “stepwise” (SW). Lee, *et al.* produced the coated SPION through both methods and examined results to determine which method was better for the desired outcome. They found that the IS-SPION created smaller sizes and lower magnetization. The SW method produced the needed size of the SPION with higher magnetization levels. In both methods, polymer coating resulted in the hydrophilic PEG being present at the outer surface of the SPION as desired. The hydrolyzed silane formed multiple covalent bonds at the surface of the magnetite. Cross-linkage between silane groups of the polymer chains resulted in hardening of the layers of copolymers. The representation of the poly(TMSMA-*r*-PEGMA)@SPION is shown in Figure 1.⁸

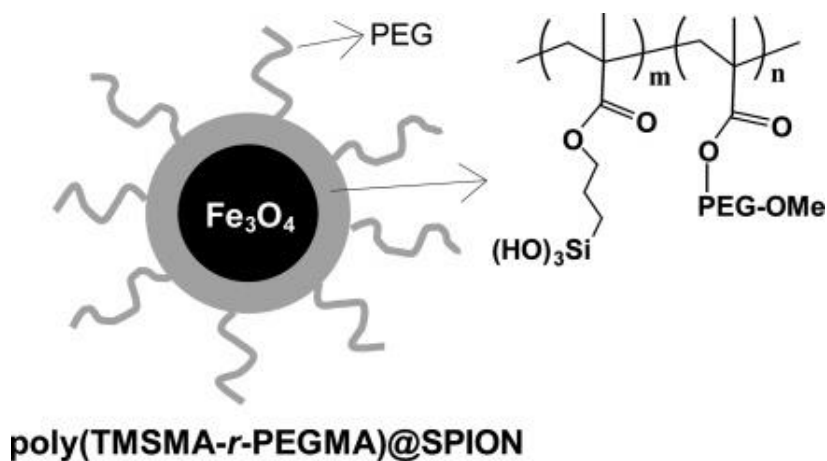


Figure 1: A representation of the polymer-coated SPION and the chemical structure of the poly(TMSMA-*r*-PEGMA) are depicted.⁸

To examine the formation of the poly(TMSMA-*r*-PEGMA)@SPION, Fourier transform infrared spectroscopy (FTIR) was used. Spectra were taken for both the IS-SPION and the SW-SPION. The spectra, found in Figure 2, showed peaks around 1720, 1105, and 627 cm^{-1} that

correspond to a carbon to oxygen double bond, carbon to oxygen single bond, and a silicone to oxygen single bond, respectively. These bonds are some of the identifiable aspects that confirm the presence of the poly(TMSMA-r-PEGMA) attached to the SPION.⁸

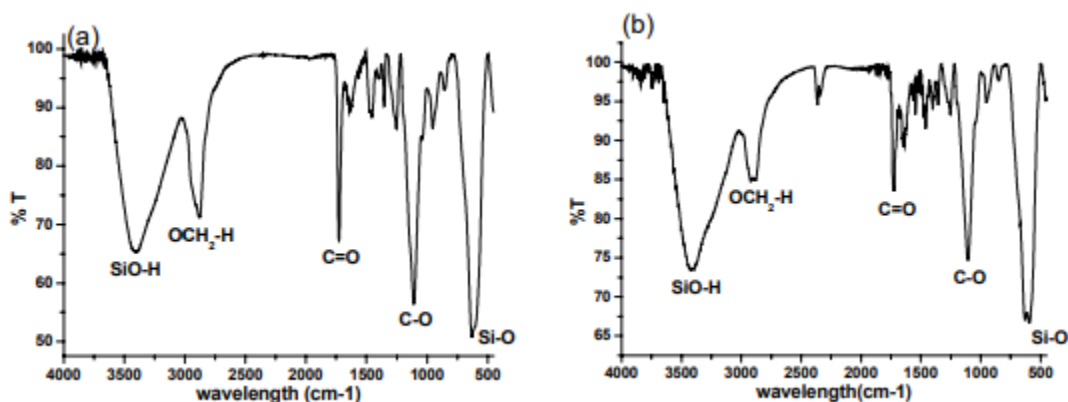


Figure 2: The Fourier transform infrared spectroscopy results of both the (a) IS-SPION and (b) SW-SPION are shown with important peaks labeled with the corresponding bonds.⁸

Thermogravimetric analysis (TGA) was used to reveal that the weight percentage of the poly(TMSMA-r-PEGMA) was 45% for IS-SPION and 30% for the SW-SPION. Dynamic light scattering (DLS) measurements showed narrow size distributions for both SPIONs. This means that there is uniformity within the nanoparticles and that production seems to create SPIONs in a consistent manner. Transmission electron microscopy (TEM) images indicate that the core size of the SW-SPION is greater than that of the IS-SPION. From this information and the results from the DLS, it can be concluded that the SW-SPION has a thinner coating of the polymer layers than the IS-SPION. This corresponds with the data from the TGA.⁸

As mentioned before, the method for creating the IS-SPION can cause lower magnetization because of the interference of the polymer in the crystallization step of iron oxide

nanoparticles. When testing the magnetic moment of both nanoparticles, it was found to agree with this hypothesis as the SW-SPION showed a larger magnetic moment than the IS-SPION. The magnetic moment measured for the SW-SPION was larger than any previously reported polymer-coated SPION of this size. This is one potential advantage of the SW method over the IS coating method.⁸

Stability tests needed to be conducted before the research went any farther. The SPION were investigated in phosphate buffered saline (PBS) over a broad pH range to mimic physiological conditions. Neither SPION showed aggregation in the pH range from 1 to 10 over a span of 1 month. The naked SPION exhibited aggregation within the first hour. This implies that the polymer coating allowed the SPION to remain suspended in aqueous media.⁸

Another aspect of the SPION that Lee, *et al.* investigated was the uptake of the nanoparticles by macrophages. Cell uptake experiments were run using a macrophage cell line. To detect the presence of SPION within the cells, Prussian blue staining was performed after 2 hours. The SPION uptake was compared to Feridex I.V., a common MRI contrast agent. The uptake of Feridex I.V. was high and most of the cells were blue after the staining. IS- and SW-SPION showed a significantly lower amount of uptake by the cells. This can be seen by the low amount of blue staining in the cells in Figure 3. The decreased uptake of the IS- and SW-SPION seems to indicate that the polymer coating layer in this system is able to greatly minimize the recognition by macrophages.⁸

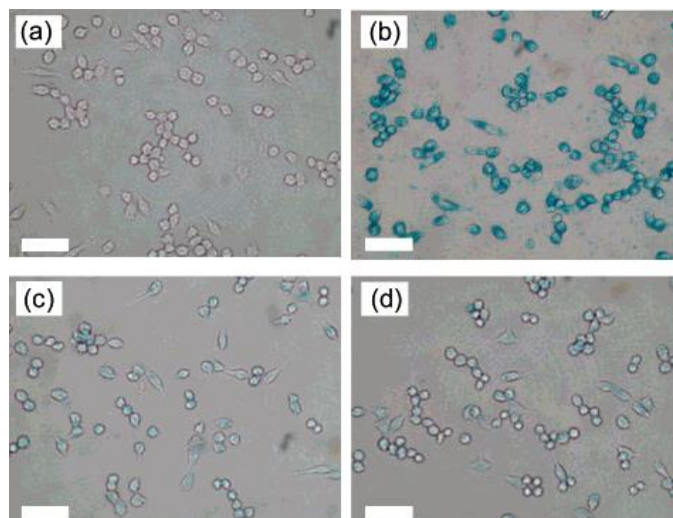


Figure 3: Prussian blue staining images of a macrophage cell line are depicted. (a) The control cells with no blue staining are shown. (b) The cells treated with Feridex are shown to contain high levels of Prussian blue. (c) Cells treated with IS-SPION and (d) those treated with SW-SPION both show low levels of Prussian blue.⁸

The toxicity of the poly(TMSMA-r-PEGMA)@SPION was then examined within the Lewis lung carcinoma (LLC) cell line by performance of an MTT assay. Even at high concentrations, the SPION shows no toxicity. The tests were ran using concentrations as high as 100 μg of iron per mL. This concentration is much higher than those needed for conventional SPION-based MRI contrast agents. The use of the poly(TMSMA-r-PEGMA)@SPION should be a safe option for use within the body as an MRI contrast agent.⁸

Lee, *et al.* hypothesized that poly(TMSMA-r-PEGMA)@SPION could accumulate within the tumor sites by the enhanced permeability and retention (EPR) effect. This is possible because of the presence of leaky vasculatures in and around tumors. The increased hyperpermeability allows the SPION to be brought into the tumor. This hypothesis was tested by subcutaneous injection of the LLC cell line into mice, followed by MR imaging of the mice at

specific time points. The tumors were visible as hyperintense areas in the MR images found in Figure 4. It was found that IS-SPION were removed from tumors much faster than the SW-SPION. This may be attributed to the smaller size of the SW-SPION. The SW-SPION allowed the tumor to still be visible for up to 4 hours after injection, with all of the nanoparticle removed from the tumor site after 11 hours. Some nanoparticle accumulation occurred within the kidneys but was gone within a day. This would seem to indicate that the SPION is able to be removed from the system in a way that should not allow any harm to be done.⁸

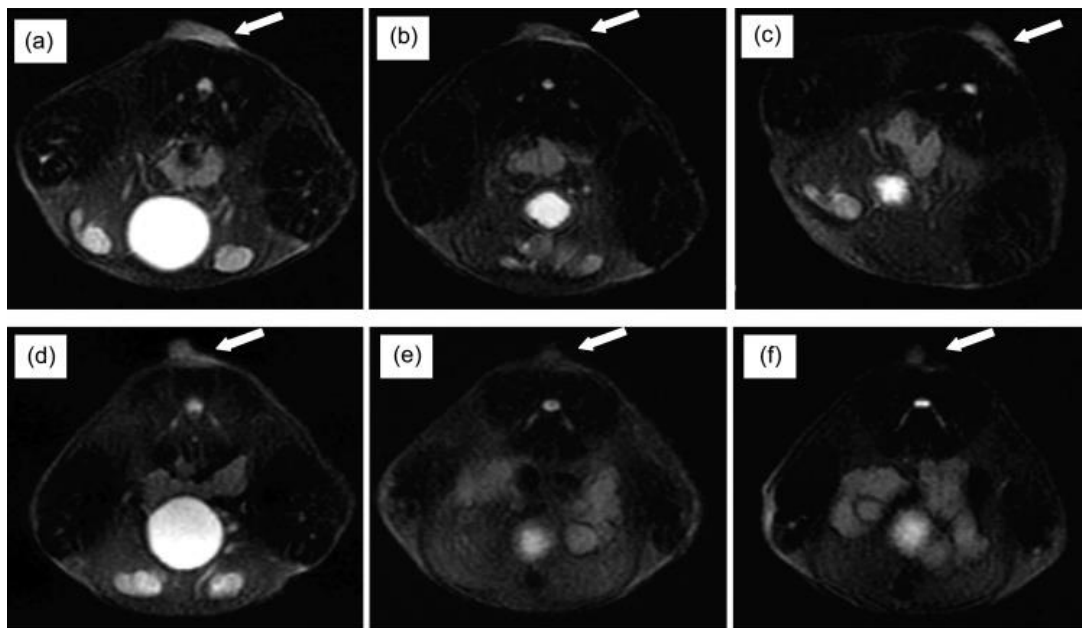


Figure 4: MR images taken at 0,1 and 4 hours post injection using IS-SPION (a, b, and c) and SW-SPION (d, e, and f).⁸

Prussian blue staining of the tumors was also performed to identify any accumulation of iron oxide within the tumor areas. Larger amounts of iron oxide were present within the tumors of the mice that had been injected with the SW-SPION than in the mice injected with IS-SPION. This matches the results of the MR images. The staining and MR images show that the

poly(TMSMA-*r*-PEGMA)@SPION is able to successfully target the tissue from tumors to allow for cancer imaging and diagnosis.⁸

The poly(TMSMA-*r*-PEGMA)@SPION work as antifouling nanoparticles to be used for cancer imaging and diagnosis. These nanoparticles showed *in vivo* magnetic resonance imaging capabilities and can potentially be used as a cancer diagnostic method. The SPION were able to enter tumor tissues directly via the EPR effect and resist uptake by macrophages. The targeting efficacy of these magnetic nanoproboscopes could potentially be increased by attaching specific targeting ligands onto the surface. Further research can be done into this and the ability to replicate these results in larger organisms.⁸

pH-Responsive Metal Organic Framework Nanoparticles Used for Treatment

Protein therapy has arisen as a great potential treatment for various diseases. The design and delivery of the proteins are typically challenging as they are poor at permeating the cell membrane and are susceptible to denaturation. Scientists have begun integrating proteins with molecules that have a greater ability to penetrate cell membranes and protect them from degradation.¹⁰ The problems associated with any of the past polymeric capsules used for protein transport are the loading efficiency and capacity limiting the effectiveness for therapeutic use and the high level of removal by phagocytes.

Cheng, *et al.*, introduced the concept of a biomimetic nanosystem that encapsulates proteins in a metal organic framework (MOF) nanoparticle camouflaged by an extracellular vesicle membrane (EVM) as depicted in Figure 1. The desire was to encapsulate the protein in a MOF that would allow for intracellular release. An EVM would then be added to protect the MOF and protein from phagocytes.

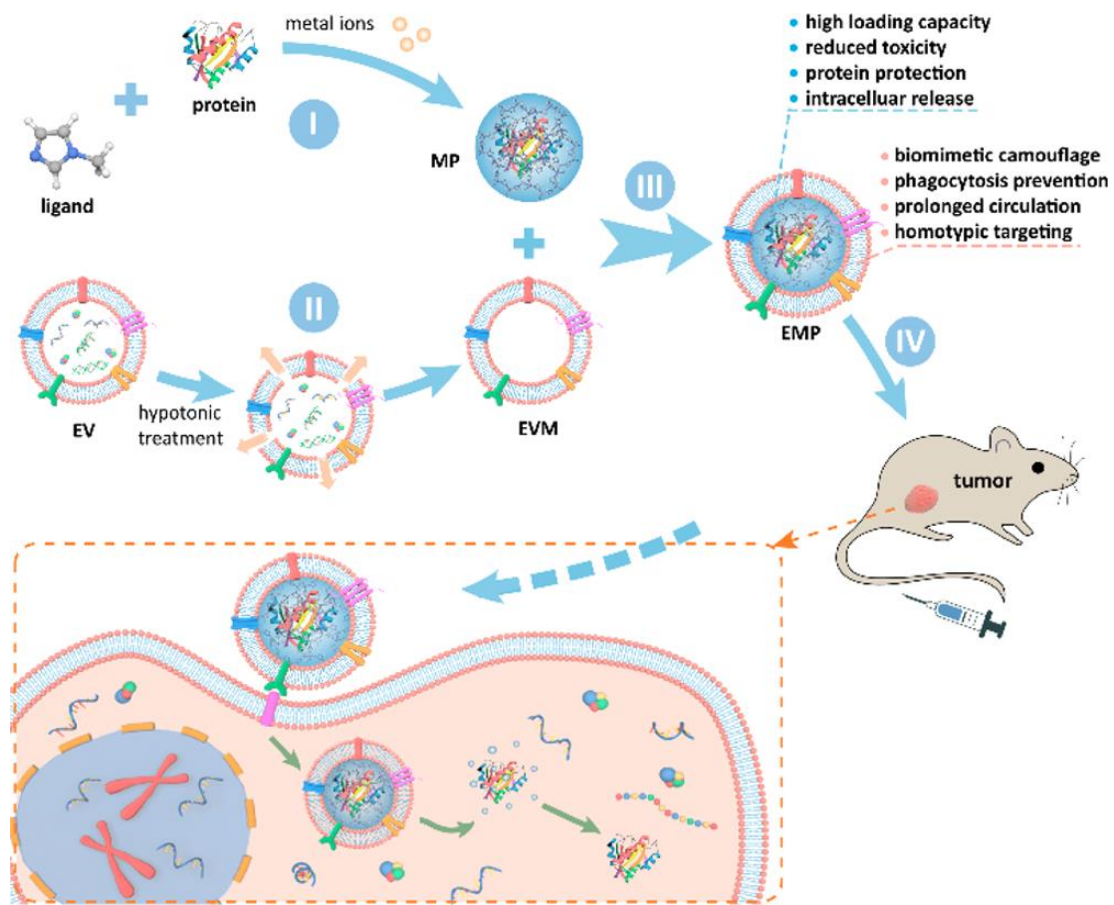


Figure 5: A schematic that illustrates the approach used to create the biomimetic EMP nanoparticle used for targeting tumors and delivering anticancer proteins into the cells.¹¹

The MOF used is the zeolitic imidazolate framework-8 (ZIF-8). Cheng, *et al.*, used the ZIF-8 matrix to encage proteins by the assembly of metal nodes of Zinc ions with 2-methylimidazole.¹¹ The MOF of this complex is pH-responsive as the metal-ligand bonds release the proteins in an acidic environment. This makes it possible for the MOF to release the proteins within endosomes or lysosomes in cells. The internal surface area of the MOF-protein (MP) nanoparticles is large, and this, in combination with the noncovalent affinity, allows a high amount of protein to be loaded within it. The loading efficiency is about 94%.¹¹

The protein cargo is enveloped by the ZIF-8 nanoparticles by self-assembly as an aqueous solution, while adjusting the concentration of the ligands and proteins to optimize the diameter and morphology of the MP nanoparticles. Various proteins were able to be encapsulated in MP nanoparticles without altering the crystal structure or morphology of the MOF. The major factors that impacted whether a protein caused a change in the morphology were the isoelectric points and the molecular weight. To test the ability of the MP nanoparticles to encapsulate the proteins, Fourier transform infrared spectroscopy (FTIR) was used. Peaks around 1667 cm^{-1} were observed if the proteins were absorbed by the MOF as this would indicate a carbon to oxygen double bond. The spectra presented in Figure 6 show the FTIR results from the protein the MOF and the MP separately. The arrow points to the peak present in the spectra for the MP that matches the needed 1667 cm^{-1} . The pore size of the MOF helps stop proteases from gaining access to the engaged proteins.

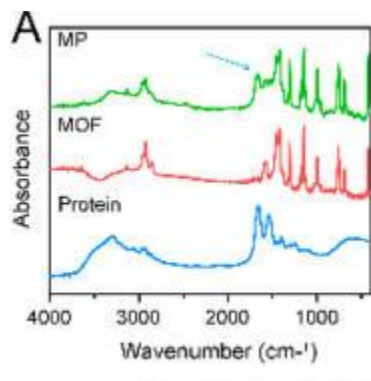


Figure 6: Fourier transform infrared spectroscopy results from the protein, MOF, and MP are shown. An arrow points to the key bond used to confirm the encapsulation of the protein by the MOF.¹¹

The MP nanoparticles were then coated in extracellular vesicles. The EVs were obtained from tumor cells by ultracentrifugation. The EVM is assembled around the MP nanoparticle

surface with the assistance of ultrasonication.¹¹ Success of this method could be partially driven by electrostatic and hydrophilic interactions between the EV membrane and the MOF matrix.¹² The process was optimized to where the EVM could completely cover the surface of the nanoparticle. Most of the content from the EV that had the chance of causing tumor metastasis was removed throughout the course of this procedure. The use of tumor-cell-derived EVs allows the preferential targeting of cancer cells from great distances within the organism. This was shown to be true by testing the EMP nanoparticle that had an EVM derived from MDA-MB-231 tumor cells on various cell lines. The uptake of the EMP nanoparticles by the MDA-MB-231 cells exhibited an uptake efficiency about 2- to 8-fold higher than the other cells tested.¹¹

The stability of the EMP nanoparticles was then tested. Dynamic light scattering, a technique commonly used for determining particle size and size distribution studies,¹³ was used, as well as TEM. After three days, there was no significant change in the EMP nanoparticles. The stability can be attributed to the hydrophilic surface glycans of the membrane. The hydrophilicity allows the EMP nanoparticles to be dissolved in aqueous solutions within the body.¹¹

The fate of nanoparticles within an organism is determined by the ability of the nanoparticles to adsorb proteins. The EMP nanoparticles have been designed to have a reduced amount of adsorption of serum proteins. The EVM portion of the EMP nanoparticles allows for a reduced adsorption of serum proteins because of the hydrophilic surface glycans. This allows an approximately 6-fold reduction in the adsorption of proteins compared to the bare MP nanoparticles. Another major factor in the survival of the biomimetic nanoparticles is the ability to avoid internalization by macrophages. To test the EMP nanoparticles for this, fluorescence proteins were encapsulated in the nanoparticles and allowed to incubate in a macrophage-like cell line for 2 hours. Using laser scanning microscopy and flow cytometry, Cheng, *et al.*, were

able to see a decrease in the uptake of the proteins into the macrophage-like cells compared to MP nanoparticles and liposome-enveloped nanoparticles. The uptake into the macrophage-like cells of EMP nanoparticles was only about 30% that of the original MP nanoparticles.¹¹

The uptake and intracellular release mechanisms of the EMP nanoparticles were also studied. One of the most common methods to allow particles into a cell is known as endocytosis. To study the mechanism of internalization for the EMP nanoparticles, the cells that were treated were also incubated in various endocytosis inhibitors. Flow cytometry results indicated that inhibitors dynasore and methyl-beta-cyclodextrin caused the uptake of the nanoparticles to be greatly reduced.¹¹ This showed that the internalization of the EMP nanoparticles happens via dynamin- and cholesterol-dependent endocytosis.¹⁴ The nanoparticle was wrapped inside of an endosome as it enters the cell.

Once inside of the cell, the EMP nanoparticle's pH dropped. The addition of hydrogen ions into the inside of the endosome attributes for this. The decreased pH causes the MOF matrix to release the organic ligand of the imidazole derivative. The proteins are released inside of the endosome as well. This causes a buffering effect as the imidazole ring becomes protonated.¹¹ This cationic polymer leads to osmotic swelling of the endosome, which results in the breaking of the endosomal membrane and the release of the proteins into the cytosol. The mechanism described is known as the "proton-sponge" effect.¹⁵

These EMP nanoparticles then had the protein gelonin, an *N*-glycosidase that cleaves a bond in rRNA that inhibits protein synthesis, enveloped within them. This combination was then tested on MDA-MB-231 cells *in vitro*. While the MOF nanoparticles and the EVM-enveloped nanoparticles have no significant levels of toxicity without the protein, the EMP nanoparticles

loaded with gelonin and the MP nanoparticles that contain gelonin show high levels of cytotoxicity to the cancerous cells. The EMP nanoparticle shows a half-maximal inhibitory concentration of about 0.025 μM . The half-maximal inhibitory value, or IC_{50} value, is a measure of the concentration that is required to inhibit 50% of the cells from growing. The smaller the value is, the more toxic the compound is.¹¹

The combination of EMP nanoparticles with gelonin was then tested on tumors in mice and compared to treating the tumors separately with just phosphate buffered saline solution, gelonin, and the MP nanoparticles. The EMP nanoparticle treated tumors showed decreased tumor growth compared to any of the other controls. The results can be seen in Figure 7. Mice were then dissected and the cells from throughout the body were examined. None of the major organs showed any abnormalities after being treated with any of the four options, including the EMP nanoparticles. The EVM-camouflaged EMP nanoparticles can target tumor tissue and inhibit growth while causing minimal toxicity in other major organs. The EMP nanoparticles, loaded with an indocyanine green-labeled gelonin, accumulated at the tumor site according to fluorescent scans. The levels of fluorescence in other parts of the mice were detectable within the first 24 hours but were nonexistent after 72 hours. This shows that the nanoparticle was able to pass through the rest of the body and only target the cancer cells.

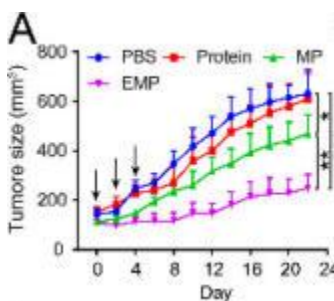


Figure 7: Tumor growth was greatly diminished by treatment with gelonin encapsulated by EMP nanoparticles.¹¹

The EMP nanoparticle developed by all-in-one self-assembly shows high levels of loading efficiency combined with high cancer targeting. The ability of the EMP nanoparticle to deliver proteins directly to the cancerous cells due to the extracellular vesicle membrane camouflage is possibly translational. Using the protein gelonin as a model, Cheng, *et al.*, were able to show that the EMP nanoparticles were able to deliver proteins to cancerous cells while going mostly undetected by the cell immune responses.¹¹ This shows a promising use for cancer treatment as the EMP nanoparticles could potentially deliver proteins to any cell in the body.¹¹

Trimodality Imaging and Treatment Using an Upconversion Nanoparticle

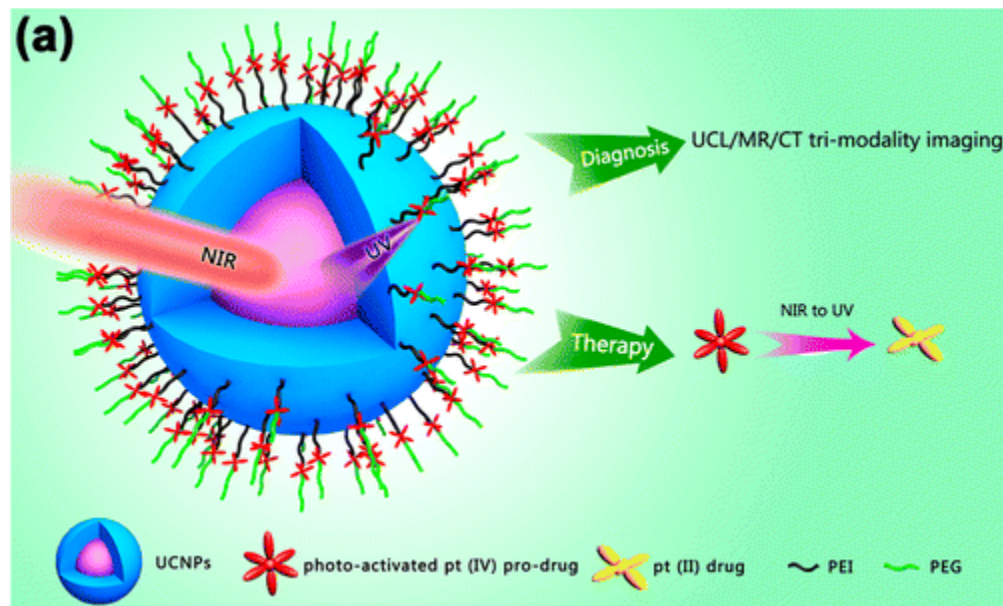


Figure 8: Upconversion nanoparticles work by converting NIR light into the UV. This can be used for diagnosis or therapy.¹⁶

Some nanoparticles can work as an imaging method for cancer and a treatment. One such nanoparticle that is being studied works for imaging cancer and is able to deliver a drug used to treat it. The possibility of a hybrid system that combines multiple diagnosis methods and therapy drugs together has become more likely with the emergence of greater nanotechnology. Different imaging techniques are used to diagnose cancer, but they all have limitations. For instance, MRI provides great spatial images but has limited sensitivity.¹⁷ Taking advantage of multiple imaging systems together can increase the abilities for cancer diagnosis.

The nanoparticle studied by Dai, *et al.* is a trans-platinum pro-drug-conjugated upconversion nanoparticle.¹⁶ Upconversion luminescence (UCL) is a nonlinear optical process that converts low-energy photons that are in the near infrared (NIR) end of the spectrum into high-energy photons that are in the ultraviolet (UV), visible or NIR by the sequential absorption of two or more photons. This process causes a large Stokes shift and sharp emission lines.¹⁸ Various lanthanide doped upconversion nanoparticles have been used for deep tissue imaging and as contrast agents for magnetic resonance imaging (MRI) and computer tomography (CT).¹⁹ The hope of Yunlu Dai, *et al.* was to develop an upconversion nanoparticle-based multimodal imaging technology that is also able to deliver chemotherapy.¹⁶

Trans-Platinum(IV) complexes have been shown to be activated to higher toxic platinum(II) complexes by UV, green or blue light.²⁰ The use of these shorter wavelengths of light are not sensible to use *in vivo* as these have poor penetration into the tissue and cause damage to healthy tissue. Dai, *et al.* attempted to solve these issues by creating an Ytterbium/Thulium-co doped upconversion nanoparticle. This nanoparticle emits UV via multiphoton absorption of NIR light. The hope is that the nanoparticle will be able to effectively be upconverted as NIR light has the deepest tissue penetration of all safe wavelengths of light.¹⁶

The upconverted nanoparticle created by Dai, *et al.* has a core shell of NaYF₄:Yb³⁺/Tm³⁺@NaGdF₄/Yb³⁺ (UCNPs) that acts as the drug carrier. This was created by a thermal decomposition method. The product from this step is then stabilized using polyethylenimine (PEI). The dicarboxyl light-activated platinum(IV) pro-drug used is trans,trans,trans-[Pt(N₃)₂(NH₃)(py)(O₂CCH₂CH₂COOH)₂] (labeled as DPP). The UCNPs were enhanced with the DPPs being conjugated to their surface by adding the PEI-UCNPs to N-hydroxysuccinimide (NHS) and 1-(3-dimethylaminopropyl)-3-ethylcarbodiimide hydrochloride (EDC). NHS is used as a carboxylic acid activator and EDC is a carboxyl activating agent. The UCNP-DPP was then coated with a layer of polyethylene glycol (PEG). The addition of PEG is used to reduce the possibility of evoking a response to the nanoparticles from the host's immune system. The structure of the nanoparticles was confirmed using high-angle annular dark-field scanning transmission electron microscopy. Results from the high-angle annular dark-field scanning transmission electron microscopy (HAADF-STEM) show that the platinum(IV) pro-drug was successfully conjugated on the surface of the nanoparticles.¹⁶

To examine whether this process worked to create the UCNP-DPP-PEGs, transmission electron micrographs were taken as shown in Figure 9. The UCNPs show uniform morphology and a size around 65 nm. The phase structure of the nanoparticles was examined using X-Ray diffraction. The results confirmed the structure of the nanoparticles to have a core pattern of a hexagonal phase structure of NaYF₄. The growth of the NaGdF₄ shell is shown as well. When the NaGdF₄ increased the upconversion luminescence intensity increased remarkably. Inductively coupled plasma mass spectrometry (ICP-MS) was utilized to find that the platinum content of the nanoparticles is 26 µg per mg of UCNP-DPP-PEG.¹⁶

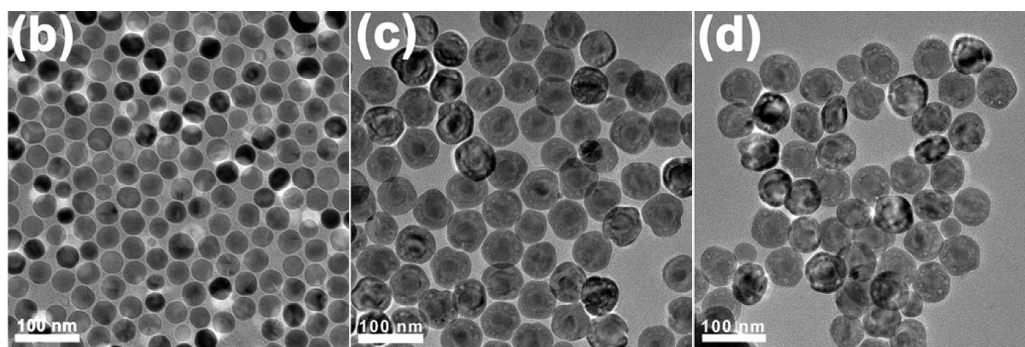


Figure 9: Transmission electron microscope images of the oleic-acid-capped nanoparticles (b), core-shell structured UCNPs (c), and UCNP-DPP-PEG nanoparticles (d).¹⁶

Tm³⁺-doped UCNPs can emit NIR light at 800 nm after excitation from a 980 nm laser. This emission can be used to cause the NIR-to-NIR UCL imaging as the UCNPs emit in the UV, visible and NIR. The UCNP-DPP-PEGs were injected into tumors in mice. The UCL imaging confirmed that a significant signal could be produced and observed from use of the UCNP-DPP-PEG within the tumor. The Gd³⁺ ions of the UCNPs cause the UCNPs to have the ability to be used as MRI contrast agents. The UCNP-DPP-PEG also shows a greater ability for use as a contrasting agent in CT imaging than the commonly used iobitridol.¹⁶

The ability of the UCNP-DPP-PEGs to be used as a cancer treatment were also studied. The first investigation looked into whether the UV emission caused by the upconversion of the UCNPs could activate the platinum (IV) DPP. The absorption spectrum of the DPP is compared with the emission spectra of pure UCNPs and DPP-conjugated UCNPs with the use of a 980 nm laser. The decrease in the emission intensity of the UCNP-DPPs at 452 and 477 nm and the decrease in the UV range indicate that the DPP is being activated as shown in Figure 10a. The absorption spectra of the UCNP-DPP-PEG is expressed as a function of exposure time to the 980

nm laser. This spectrum decreases in intensity at 289 nm with increased exposure time as seen in Figure 10b. When platinum-azide bonds break, there should be a decrease in the spectrum at 289 nm. When the DPP is released, it is expected that there would be a loss of platinum-azide bonds.²¹ The 980nm laser effectively activates the platinum (IV) complex.¹⁶

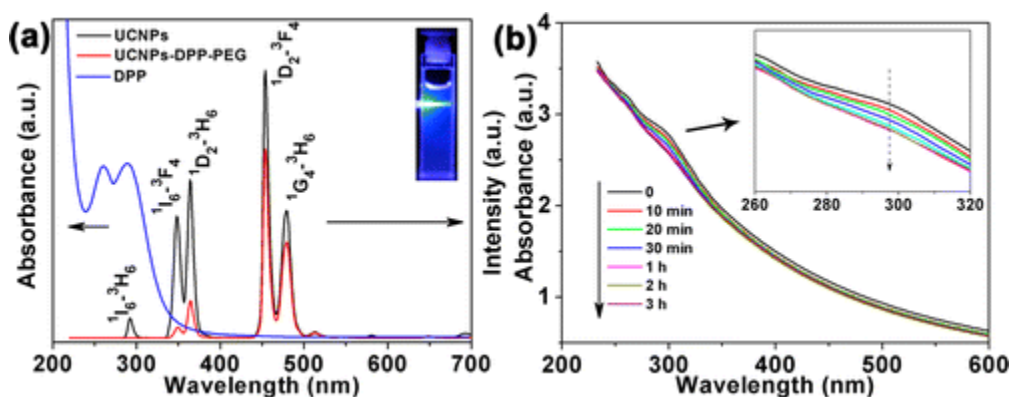


Figure 10: The absorption spectrum of the DPP and emission spectra of UCNPs and DPP-conjugated UCNPs are depicted after being introduced to NIR light from a 980 nm laser (a). The absorption spectra of the UCNP-DPP-PEG expressed as a function of time of exposure to 980 nm laser radiation with a highlight of the decrease at 289 nm (b).¹⁶

ICP-MS was performed to examine the stability of the UCNP-DPP-PEGs within the blood. Only 30% of the platinum was released into the serum after 48 hours in the dark. The ability of the UCNP-DPP-PEGs to release the DPP molecules was also calculated to be roughly between 3000 DPP molecules per UCNP-DPP-PEG over 1 hour under a 980 nm laser. With 1 hour of irradiation from 365 nm UV light, 10000 DPP molecules are released per particle. The use of the NIR light or UV can effectively cause the upconverted UV emission from the UCNPs to convert the platinum (IV) DPP into platinum (II) complexes. These rough calculations were performed based upon the absorption spectra under the NIR and UV irradiation. The ability to

release the drug under the 980 nm NIR joined with the ability to activate the DPP to form highly toxic platinum (II) drugs increases the ability to kill cancer cells.¹⁶

To test for the cytotoxicity of the UCNP-DPP-PEGs, HeLa cells were dosed with varying concentrations of the nanoparticles. Both the control and the cells dosed with UCNP-DPP-PEGs were irradiated with the 980 nm laser or the UV light. These tests showed that the DPP complexes can be delivered via the UCNPs to the cells and can be activated to form the more cytotoxic platinum (II). The DPP conjugated UCNPs are able to reduce the adverse side effects that are normally seen from platinum-based anticancer drugs.¹⁶

The research presented by Dai, *et al.* is the first recorded example of using UCNPs as nanotransducers that also control trimodality imaging. These UCNPs convert the penetrating NIR light into UV radiation to release the anticancer drugs. The use of NIR light allows for activation of the UCNP-DPP-PEG at increased depths within the body and shows better tumor growth inhibition than using 365 nm UV radiation. Most other photodynamic therapies (PDTs) require a presence of oxygen to kill cancer cells. This is a problem as cancer cells tend to be hypoxic. The UCNP-DPP-PEG does not require the oxygen and, therefore, has a more promising application as a cancer therapy. Further research will be conducted by this group into the mechanisms of the reactions that happen in the UCNP-DPP-PEGs and into the ability to inject the nanoparticles intravenously.¹⁶

Glycopolymer-Stabilized Gold Nanoparticles for Use as a Cancer Vaccine

Another nanoparticle that has been researched recently takes a different approach to treating cancer. Parry, *et al.* worked to produce a nanoparticle-based cancer vaccine. Two types of cancer vaccines exist. Preventative cancer vaccines work in a similar method to the influenza

vaccination, but the treatment cancer vaccines work as another method to attack the cancer once it has already formed.²² The synthesized nanoparticle investigated would work as a preventative vaccine to protect the patient from breast cancer.²³

Healthy mammary cells have a surface that is characterized by branched, O-linked glycans. These glycans have high levels of a compound called N-acetyl-D-glucosamine (GlcNAc). Breast cancer cells present linear, truncated mucin-type glycans. Mucin-type glycans are carbohydrates that form a thin layer similar to mucus. An example of the type of glycan present on the membrane of breast cancer cells is α -N-acetyl- D-glucosamine (α GalNAc). This glycan is also known as the Tn-antigen ligand.

The hope of Parry, *et al.* was to create a nanoparticle that presents a surface like that of breast cancer cells to engage the receptors of the immune system. This would produce an effective vaccine. Other attempts to perform this included using peptides²⁴, dendrimers²⁵ and proteins. The alternative platform of the nanoparticle offers greater synthetic controls and increased density of glycans compared to any of the current scaffolds produced. Presenting the carbohydrates in a “multicopy-multivalent” manner on the surface of the nanoparticle should create a surface that mimics that of a cancerous cell.²³ The “multicopy-multivalent” manner is simply placing the same glycan on the surface multiple times in a row to offer more locations for antigens or antibodies to bind.²⁶ Figure 11 shows the reaction used to create the desired Tn

glycan monomer with the correct stereochemistry.

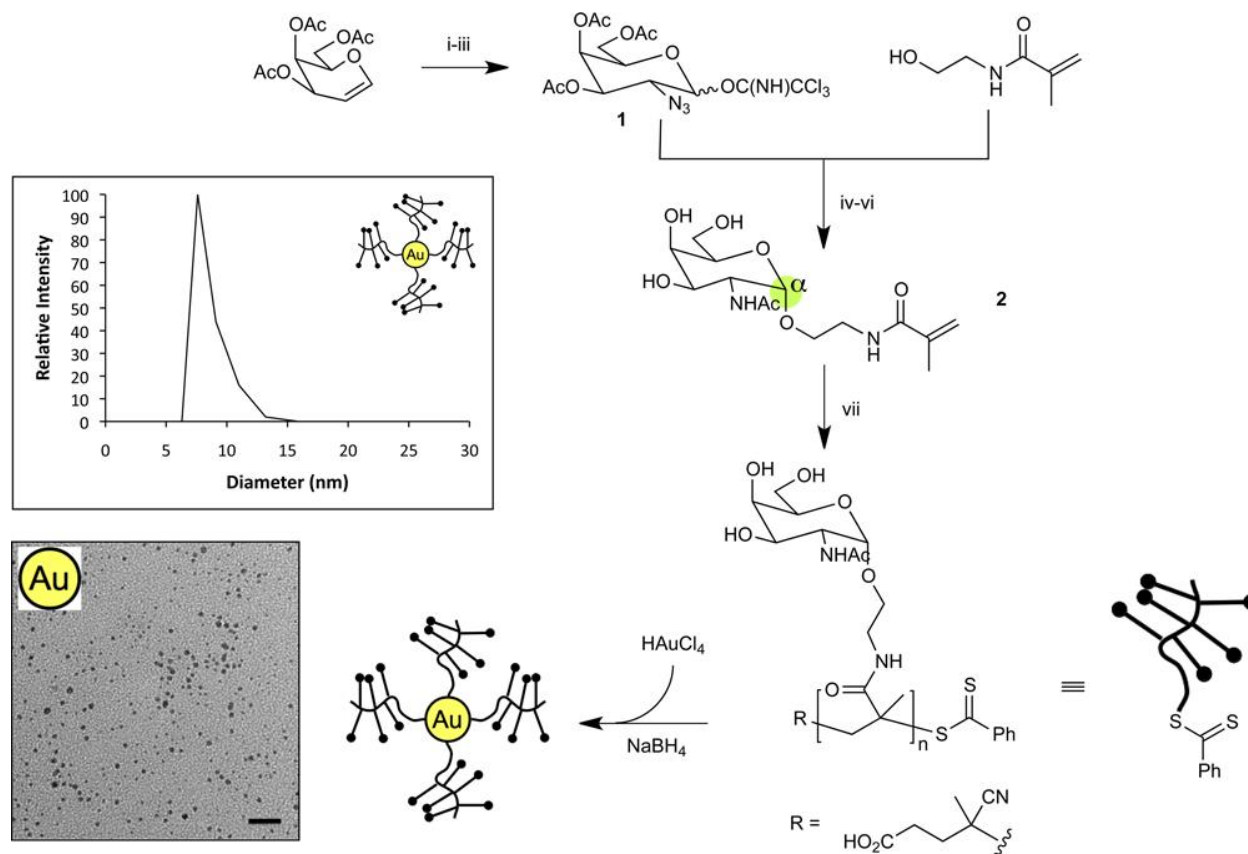


Figure 11: A presentation of the reaction pathway to create the glycopolymer-stabilized gold nanoparticles. The size of the nanoparticles produced show consistency, with a diameter around 9 nm.²³

Once the pure anomer had been created, the glycopolymers were prepared using a process known as Reversible Addition-Fragmentation chain Transfer (RAFT) polymerization.²³ This is a radical polymerization that uses a chain transfer agent that allows for control over the length of the chain and the polydispersity of the polymer.²⁷ By varying the ratio of reactants and conditions, chains of various lengths and compositions were obtained. The Tn-antigen glycan

monomer was then copolymerized with poly(ethylene glycol) methyl ether methacrylate (PEGMA). These polymers were then added to the gold nanoparticle via a reduction by sodium borohydride to form the polyTn-NPs.²³

The size of the nanoparticles was tested using dynamic light scattering and transmission electron microscopy. The size distribution of the particles presented diameters mostly in the range of 5 to 20 nm. To test the loading of the antigen and the polymer, TGA was used. The results indicated that longer polymer chains could be used to create smaller nanoparticles with a larger ratio of glycans to gold.²³

With the hope of Parry, *et al.* being to produce an immune response using these nanoparticles, tests had to be ran *in vivo* on New Zealand White rabbits. The rabbits were immunized with the polyTn-NP or free polymers at various times throughout the testing. An ELISA assay was performed on blood drawn from the rabbits at day 0, 42 and 70 to test for the number of antibodies present. The results from the rabbits that were treated with just the free polymers showed low or negligible responses from the immune system as very few antibodies were produced, as can be seen in Figure 12. All the rabbits treated with the glyconanoparticles had a greater concentration of antibodies present. The number of antibodies also increased as time went on.²³

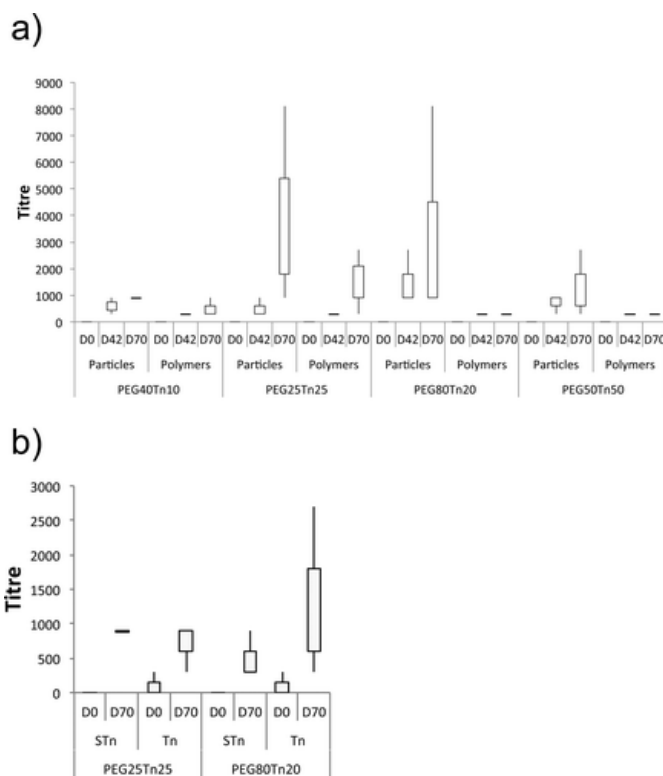


Figure 12: The results of immunological experiments with the glyconanoparticles and glycopolymers displayed as box plots. (a) Serum antibody titers were measured using the enzyme-linked immunosorbent assay (ELISA). (b) The cross-reactivity of serum antibodies with mucins were tested via ELISA.²³

Examining the data from the ELISA assays, a relationship between the density of the carbohydrates and the response from the immune system can be defined. The optimum density can be calculated to be somewhere between 20 to 25 units per polymer chain. The reason for this is not fully known and must be studied further. To test for the ability of the nanoparticle generated antibodies to recognize naturally occurring antigens, the bovine submaxillary mucin glycoprotein was used. After 70 days of immunization with the glyconanoparticles, antibodies that were specific for the naturally occurring mucin glycans were present.²³

Parry, *et al.* were able to synthesize a ‘multicopy-multivalent’ nanoparticle covered in tumor-associated antigen glycans. The nanoparticle was shown to generate significant immune responses *in vivo*. The immune system was still able to recognize natural, healthy Tn-antigen glycans. This means that the nanoparticle was able to induce an immune response specifically for breast cancer cells. The level of titers reported in this research are at a level lower than those obtained with glycoconjugates that were based on protein-toxin conjugates.²⁸ Further research must be done to figure out why the levels were lower and to determine methods to increase the response by the immune system.

Summary and Thoughts

Nanoparticles offer a great option for various disease treatments. The ability to fine tune the nanoparticles offers exceptional variability and can deliver other chemical agents to assist as treatment of cells. The capability of the anticancer drug to be either encapsulated within the nanoparticle or part of the outer layer of the particle offers other unique opportunities. As this method of drug delivery is of similar size to the cells involved, this makes it easier for direct uptake into the cells. The ability to change the outside coating of the nanoparticle offers the ability to camouflage or change the targeting abilities of the nanoparticle. The makeup of the outer shell can also be controlled in such a way as to provide other effects similar to those created by the lanthanide-doping of the UCNP. Adjusting nanoparticles allow for greater ability for them to be used for cancer imaging, prevention and treatment.

Cancers vary greatly. I believe that cancer must be attacked from multiple angles to truly make advancements in stopping the loss of life to this disease. The organometallic anticancer drugs that have been used over the past few decades have worked well, but cancers are appearing

that are resistant to treatment from drugs such as cisplatin. Other treatments will be required.

While nanoparticles are most likely not the complete answer to the problem, they are being used as anticancer therapies that can treat cancers that are resistant to cisplatin.²⁹ Immunotherapy has become a promising treatment method as well, but there are still various issues with this route.

Nanoparticles have been developed to help increase immune responses to assist the body in fighting the cancer and overcome some of the barriers faced by immunotherapy.³⁰ Radiation is another common cancer treatment. The major issue associated with radiation is that healthy cells around the tumors become damaged from the treatment. Scientists have developed nanoparticles that are able to be used for radiotherapy that assist in limiting the damage done to nearby cells.³¹ Nanoparticles are able to overcome many of the issues that face current treatment methods and they offer other possible uses in the cancer field.

One of the major issues with cancer treatments involves being able to detect the cancer in time. If the cancer is caught at an earlier stage, a patient has a higher likelihood of survival. Cancer can often go undetected, even by some of our best imaging processes. The imaging process needs to continue to expand and advance. Nanoparticles can be used for this as well. One advantage that nanoparticles exhibit is the ability to be used for multimodal imaging.^{16,32} Nanoparticles similar to the UCNP may be the imaging system that allows doctors to detect cancer earlier in patients as they offer multiple methods for visualizing of tumors. The ability of nanoparticles to congregate within tumor tissue allows for increased imaging accuracy as well. The size of nanoparticles can be controlled to make them fit into the openings of cancerous cells, but they are too large to fit into regular cells. This leads to specific uptake of the particles by tumor tissue. If the nanoparticles are created with compounds that create good contrast agents, then imaging can be utilized where only the tumor tissue will be seen.

The use of nanoparticles in cancer imaging, prevention and treatment is growing. The possible combinations to make use of seem to provide an endless number of uses to be found. Preventing patients from developing cancer seems like a possibility from the use of nanoparticles. If patients do develop cancer, then nanoparticles may be a significant method to visualize and treat the cancer. The field of nanomedicine will continue to grow and develop. Nanoparticles will be part of the answer to helping prevent more deaths from cancer, but they are not the final answer. Cancer is an extremely broad set of diseases. With all of the varying types of cancer, the number of treatments or cures will need to vary just as much. Nanoparticles offer the ability to be modified in ways that allow them to be used for imaging, prevention and treatment of cancer that can hopefully be used to match the variety found within this disease. The future applications of nanoparticles within this field will continue to grow and may be an important part of the answer to save the lives of those dying from cancer.

References

- (1) Dickinson, E. Use of Nanoparticles and Microparticles in the Formation and Stabilization of Food Emulsions. *Trends Food Sci. Technol.* **2012**, *24* (1), 4–12.
- (2) Irvine, D. J.; Hanson, M. C.; Rakhra, K.; Tokatlian, T. Synthetic Nanoparticles for Vaccines and Immunotherapy. *Chem. Rev.* **2015**, *115* (19), 11109–11146.
- (3) Gouma, P. I.; Lee, J. Photocatalytic Nanomats Clean up Produced Water from Fracking. *Transl. Mater. Res.* **2014**, *1* (2), 025002.
- (4) What Is Cancer? <https://www.cancer.gov/about-cancer/understanding/what-is-cancer>.
- (5) Mantri, Y.; Lippard, S. J.; Baik, M. H. Bifunctional Binding of Cisplatin to DNA: Why Does Cisplatin Form 1,2-Intrastrand Cross-Links with AG but Not with GA? *J. Am. Chem. Soc.* **2007**, *129* (16), 5023–5030.
- (6) Martina, M. S.; Fortin, J. P.; Ménager, C.; Clément, O.; Barratt, G.; Grabielle-Madelmont, C.; Gazeau, F.; Cabuil, V.; Lesieur, S. Generation of Superparamagnetic Liposomes Revealed as Highly Efficient MRI Contrast Agents for in Vivo Imaging. *J. Am. Chem. Soc.* **2005**, *127* (30), 10676–10685.
- (7) Kurzhals, S.; Gal, N.; Zirbs, R.; Reimhult, E. Controlled Aggregation and Cell Uptake of Thermoresponsive Polyoxazoline-Grafted Superparamagnetic Iron Oxide Nanoparticles. *Nanoscale* **2017**, No. 8.
- (8) Lee, H.; Lee, E.; Kim, D. K.; Jang, N. K.; Jeong, Y. Y.; Jon, S. Antibiofouling Polymer-Coated Superparamagnetic Iron Oxide Nanoparticles as Potential Magnetic Resonance Contrast Agents for in Vivo Cancer Imaging. *J. Am. Chem. Soc.* **2006**, *128* (22), 7383–

7389.

- (9) Nie, F. Q.; Xu, Z. K.; Huang, X. J.; Ye, P.; Wu, J. Acrylonitrile-Based Copolymer Membranes Containing Reactive Groups: Surface Modification by the Immobilization of Poly(Ethylene Glycol) for Improving Antifouling Property and Biocompatibility. *Langmuir* **2003**, *19* (23), 9889–9895.
- (10) Nischan, N.; Herce, H. D.; Natale, F.; Bohlke, N.; Budisa, N.; Cardoso, M. C.; Hackenberger, C. P. R. Covalent Attachment of Cyclic TAT Peptides to GFP Results in Protein Delivery into Live Cells with Immediate Bioavailability. *Angew. Chemie - Int. Ed.* **2014**, *54* (6), 1950–1953.
- (11) Cheng, G.; Li, W.; Ha, L.; Han, X.; Hao, S.; Wan, Y.; Wang, Z.; Dong, F.; Zou, X.; Mao, Y.; et al. Self-Assembly of Extracellular Vesicle-like Metal-Organic Framework Nanoparticles for Protection and Intracellular Delivery of Biofunctional Proteins. *J. Am. Chem. Soc.* **2018**, *140* (23), 7282–7291.
- (12) Ojida, A.; Inoue, M. A.; Mito-Oka, Y.; Tsutsumi, H.; Sada, K.; Hamachi, I. Effective Disruption of Phosphoprotein-Protein Surface Interaction Using Zn(II) Dipicolylamine-Based Artificial Receptors via Two-Point Interaction. *J. Am. Chem. Soc.* **2006**, *128* (6), 2052–2058.
- (13) Liu, X.; Dai, Q.; Austin, L.; Coutts, J.; Knowles, G.; Zou, J.; Chen, H.; Huo, Q. A One-Step Homogeneous Immunoassay for Cancer Biomarker Detection Using Gold Nanoparticle Probes Coupled with Dynamic Light Scattering. *J. Am. Chem. Soc.* **2008**, *130* (9), 2780–2782.

- (14) Gilleron, J.; Querbes, W.; Zeigerer, A.; Borodovsky, A.; Marsico, G.; Schubert, U.; Manygoats, K.; Seifert, S.; Andree, C.; Stöter, M.; et al. Image-Based Analysis of Lipid Nanoparticle-Mediated siRNA Delivery, Intracellular Trafficking and Endosomal Escape. *Nat. Biotechnol.* **2013**, *31* (7), 638–646.
- (15) Behr, J. P. The Proton Sponge. A Trick to Enter Cells the Viruses Did Not Exploit. *Chimia (Aarau)*. **1997**, *51* (1/2), 34–36.
- (16) Dai, Y.; Xiao, H.; Liu, J.; Yuan, Q.; Ma, P.; Yang, D.; Li, C.; Cheng, Z.; Hou, Z.; Yang, P.; et al. In Vivo Multimodality Imaging and Cancer Therapy by Near-Infrared Light-Triggered Trans -Platinum pro-Drug-Conjugated Upconversion Nanoparticles. *J. Am. Chem. Soc.* **2013**, *135* (50), 18920–18929.
- (17) Viswanathan, S.; Kovacs, Z.; Green, K. N.; Ratnakar, S. J.; Sherry, A. D. <Alternatives to Gadolinium-Based Metal Chelates for Magnetic Resonance Cr900284a.Pdf>. **2010**, 2960–3018.
- (18) Haase, M.; Schafer, H. Upconverting Nanoparticles. *Angew. Chemie - Int. Ed.* **2011**, *50* (26), 5808–5829.
- (19) Cheng, L.; Yang, K.; Li, Y.; Chen, J.; Wang, C.; Shao, M.; Lee, S.-T.; Liu, Z. Facile Preparation of Multifunctional Upconversion Nanoprobes for Multimodal Imaging and Dual-Targeted Photothermal Therapy. *Angew. Chemie - Int. Ed.* **2011**, *123* (32), 7523–7528.
- (20) Farrer, N. J.; Woods, J. A.; Salassa, L.; Zhao, Y.; Robinson, K. S.; Clarkson, G.; Mackay, F. S.; Sadler, P. J. A Potent Trans-Diimine Platinum Anticancer Complex Photoactivated

- by Visible Light. *Angew. Chemie - Int. Ed.* **2010**, *122* (47), 9089–9092.
- (21) Mackay, F. S.; Woods, J. A.; Heringova, P.; Kasparkova, J.; Pizarro, A. M.; Moggach, S. A.; Parsons, S.; Brabec, V.; Sadler, P. J. A Potent Cytotoxic Photoactivated Platinum Complex. *Proc. Natl. Acad. Sci.* **2007**, *104* (52), 20743–20748.
- (22) Team, T. A. C. S. medical and editorial content team. Cancer Vaccines
<https://www.cancer.org/treatment/treatments-and-side-effects/treatment-types/immunotherapy/cancer-vaccines.html>.
- (23) Parry, A. L.; Clemson, N. A.; Ellis, J.; Bernhard, S. S. R.; Davis, B. G.; Cameron, N. R. ‘ Multicopy Multivalent ’ Glycopolymer-Stabilized Gold Nanoparticles as Potential Synthetic Cancer Vaccines. **2013**, No. Table 1.
- (24) Pamela Thompson, Vani Lakshminarayanan, Nitin T. Supekar, Judy M. Bradley, Peter A. Cohen, Margreet A. Wolfert, Sandra J. Gendler, G.-J. B. Linear Synthesis and Immunological Properties of a Fully Synthetic Vaccine Candidate Containing a Sialylated MUC1 Glycopeptide. *ChemComm* **2015**, No. 50.
- (25) Sven Wittrock Dr., Torsten Becker Dr., H. K. P. D. Synthetic Vaccines of Tumor-Associated Glycopeptide Antigens by Immune-Compatible Thioether Linkage to Bovine Serum Albumin. *Angew. Chemie - Int. Ed.* **2007**, *46* (27), 5226–5230.
- (26) Spain, S.; Cameron, N. R. A Spoonful of Sugar: The Application of Glycopolymers in Therapeutics. *Polym. Chem.* **2011**, *2*, 60–68.
- (27) Moad, G.; Rizzardo, E.; Thang, S. H. Toward Living Radical Polymerization. *Acc. Chem. Res.* **2008**, *41* (9), 1133–1142.

- (28) Hoffmann-Röder, A.; Kaiser, A.; Wagner, S.; Gaidzik, N.; Kowalczyk, D.; Westerlind, U.; Gerlitzki, B.; Schmitt, E.; Kunz, H. Synthetic Antitumor Vaccines from Tetanus Toxoid Conjugates of MUC1 Glycopeptides with the Thomsen-Friedenreich Antigen and a Fluorine-Substituted Analogue. *Angew. Chemie - Int. Ed.* **2010**, *49* (45), 8498–8503.
- (29) Ling, X.; Chen, X.; Riddell, I. A.; Tao, W.; Wang, J.; Hollett, G.; Lippard, S. J.; Farokhzad, O. C.; Shi, J.; Wu, J. Glutathione-Scavenging Poly(Disulfide Amide) Nanoparticles for the Effective Delivery of Pt(IV) Prodrugs and Reversal of Cisplatin Resistance. *Nano Lett.* **2018**, *18* (7), 4618–4625.
- (30) Shao, K.; Singha, S.; Clemente-Casares, X.; Tsai, S.; Yang, Y.; Santamaria, P. Nanoparticle-Based Immunotherapy for Cancer. *ACS Nano* **2015**, *9* (1), 16–30.
- (31) Dou, Y.; Guo, Y.; Li, X.; Li, X.; Wang, S.; Wang, L.; Lv, G.; Zhang, X.; Wang, H.; Gong, X.; et al. Size-Tuning Ionization to Optimize Gold Nanoparticles for Simultaneous Enhanced CT Imaging and Radiotherapy. *ACS Nano* **2016**, *10* (2), 2536–2548.
- (32) Kim, J. S.; Rieter, W. J.; Taylor, K. M. L.; An, H.; Lin, W.; Lin, W. Self-Assembled Hybrid Nanoparticles for Cancer-Specific Multimodal Imaging. *J. Am. Chem. Soc.* **2007**, *129* (29), 8962–8963.